HHS Public Access

Author manuscript

Brain Behav Immun. Author manuscript; available in PMC 2019 February 18.

Published in final edited form as:

Brain Behav Immun. 2017 May ; 62: 291–305. doi:10.1016/j.bbi.2017.02.014.

Activation of NLRP3 inflammasome by cholesterol crystalsin alcohol consumption induces atherosclerotic lesions

P. M. Abdul-Muneer[1,2], **Saleena Alikunju**[2], **Vikas Mishra**[1,2], **Heather Schuetz**[2], **Adam M. Szlachetka**[2], **Ellen L. Burnham**[3], and **James Haorah**[1,2,*]

[1]Laboratory of Neurovascular Inflammation and Neurodegeneration, Department of Biomedical Engineering, Center for Injury Bio Mechanics, Materials and Medicine, New Jersey Institute of Technology, Newark, NJ-07102.

[2]Department of Pharmacology and Experimental Neuroscience, University ofNebraska Medical Center, Omaha, NE-68198.

[3]Division of Pulmonary Sciences and Critical Care Medicine, Department of Medicine, University of Colorado School of Medicine, Aurora, CO 80045

Abstract

Epidemiological studies showed a strong association between alcoholism and incidence of stroke, for which the underlying causative mechanisms remain to be understood. Here we found that infiltration of immune cellsanddeposition of cholesterol at the site of brain artery/capillary injury induced atherosclerosis in chronic alcohol (ethanol) consumption in the presence or absence of high-fat diet. Conversion of cholesterol into sharp edges of cholesterol crystals (CCs)in alcohol intake was key to activation of NLRP3 inflammasome, induction of cerebral atherosclerosis, and development of neuropathy around the atherosclerotic lesions. The presence of alcohol was critical for the formation of CCs and development of the neuropathology. Thus, we observed that alcohol consumption elevated the level of plasma cholesterol, deposition and crystallization of cholesterol, as well as activation of NLRP3 inflammasome. Thisled to arteriole or capillary walls thickening and increase intracranial blood pressure. Distinct neuropathy around the atherosclerotic lesions indicated vascular inflammation as an initial cause of neuronal degeneration. We demonstrated the molecular mechanisms of NLRP3 activation and downstream signaling cascade event in primary culture of human brain arterial/capillary endothelial cells in the setting of dose-/time-dependent effects of alcohol/CCs using NLRP3 gene silencing technique. We also detected CCs in blood

*Corresponding author: James Haorah, PhD, Department of Biomedical Engineering, New Jersey Institute of Technology, Newark, NJ 07102. james.haorah@njit.edu.

AUTHORS CONTRIBUTIONS:

PMAM carried out the studies, performed the acquisition data and involved in manuscript preparation.SA assisted PMAM in experiments and data acquisition. AMS performed the animal care, pair-feeding, and assisted PMAM for animal surgery. VM and HS performed the kinetics of CCs formation with dose-dependent ethanol or cholesterol concentrations, and detection of CCs in blood samples. JH designed the whole project, supervised the execution of the experiments, data interpretation and prepared the manuscript. All authors read and approved the final manuscript.

COMPETING INTERESTS:

The authors have declared that no competing interests exist.

samples from alcohol users, which validated the clinical importance of the findings. Finally,combined therapy of acetyl-L-carnitine and Lipitor® preventeddeposition of cholesterol, formation of CCs, activation of NLRP3, thickening of vessel walls, andelevation of intracranial blood pressure. We conclude thatalcohol-inducedaccumulation and crystallization of cholesterol activates NLRP3/caspase-1in the cerebralvessel that leads to early development of atherosclerosis.

Keywords

Alcohol-induced cholesterol crystals; NLRP3 inflammasomes; cerebral atherosclerosis; intracranial blood pressure; therapeutic intervention

INTRODUCTION

Stroke is the third leading cause of death and the most prevalent cause of permanent disability in the world[1]. Epidemiological studies revealed that chronic alcohol consumption is associated with hypertensive atherosclerosis[2,3].Heavy chronic alcohol use accounts for about 40% of atherosclerotic strokes in western countries, similar to the prevalence of stroke in diabetes[4,5].The relevant molecular and cellular mechanisms of brain atherosclerotic lesions associated with alcohol intakeremain to be understood. We have previously demonstrated that oxidative damage of the blood-brain barrier (BBB) elicited by long-term moderate alcohol exposure and subsequent induction of inflammatory matrix metalloproteinases (MMPs) is a risk factor for cerebral vascular stroke[6,7]. Thealcohol-induced impairment of the BBB integrity is mediated by intracellular calcium signaling pathwaysvia the oxidative injury of the cerebral vasculature[8]. This oxidative injury of the brain arterial/capillary is not easily repairable because activation of MMPs by ethanol (EtOH) leads to degradation of vascular endothelial growth factor receptor-2 (angiogenesis molecule) and BBB tight junction proteins that promote atherosclerosis[9]. Thus, reduction of oxidative stress appears to be an effective measure to prevent the loss of cerebral vascular functional integrity and neurodegeneration around the perivascular region in the setting of alcoholconsumption[10,11].

On the other hand, chronic alcohol consumption has been shown to increase theabnormal levels of plasma fatty acids, triglycerides, or cholesterol that are potential risk factors for atherosclerosis [12,13]. We have shown that activation of phospholipase A2 (a phospholipid hydrolyzing enzyme to generate long chain fatty acids or cholesterol synthesis) by alcohol is critical for initiation of onsite neuroinflammation depending on the metabolic fate of these fatty acids[14]. While chronic inflammation is recognized as a pivotal role in the development of atherosclerosis [15]. Here, we link chronic alcohol consumption as the likely mediator of cerebral atherosclerotic lesions through interconnected pathways of alcohol being a potent inducer and producerof oxidative damage[7], which paves the path for immune cells infiltration (inflammatory site) as well as the site of cholesterol deposition. Our present studies demonstrate that the deposited cholesterol in the cerebral vasculature is crystallized intothe sharp edges of cholesterol crystals (CCs).

Cholesterol crystals are known to activate NLRP3 inflammasome, a marker for atherosclerosis, which appears to be regulated through oxidative stress-responsive

transcription factor Nrf2[16–18].NLRP3 (nucleotide-binding domain leucine-rich repeat containing family, pyrin domain containing 3) inflammasomes are cytosolic protein complexes [18] that are involved in immune cell activation [19]. The oligomerizaton of NLRP3 receptorcauses recruitment of caspase-1 through the adaptor protein ASC (apoptosis-associated speck-like protein) to form the active NLRP3 inflammasomes [20], which in turn activatescaspase-1 enzyme for the proteolytic cleavage of pro IL-1to active IL-1[21].

In these studies, we demonstratedthe immune cell aggregation, cholesterol deposition and crystallization, and NLRP3 inflammasomes activation at the cerebral vasculature. Atherosclerotic lesions and neuropathy surrounding the perivascular region at the site of cholesterol crystallization were observed in ouranimal model of stroke in chronic alcohol consumption. Our unique animal model [22] featureda miniature pressure catheter implantation into the right common carotid artery (CCA) of a rat without obstruction of cerebral blood flow (suppl. Fig 1). This enabledus to measure the intracranial blood pressure in a long-term survival after stroke without ligation, unlike conventional occlusion models[23]. As in real life, the atherosclerotic stroke is caused by alcohol-elicited immune cell aggregation, cholesterol deposition, CCs formation, NLRP3 inflammasomes activation, and narrowing of the brain capillariesduring chronic alcohol consumption. Using this animal model of human disease, we also tested the efficacy of a combinedtherapy of acetyl-L-carnitine (ALC) and atorvastatin in preventing the induction of oxidative stress, cholesterol deposition, CCs formation, NLRP3 inflammasomes activation, and atherosclerotic lesions in chronically alcohol diet ingested rats. ALC is effective in preventing cerebral vascular oxidative injury and mitochondrial damage by stabilizing antioxidants, and effective in lowering triglyceride build up via the -oxidation of fatty acids[11,24]. Lipitor® (atorvastatin, AVS), is an FDA-approved drug used in stroke managementthat inhibits cholesterol synthesizer coenzyme A reductase [25,26].We also tested the role of high-fat diet (HD) here to determine if HD exacerbates the levels of cholesterol and CCs formation in the setting of alcohol consumption. Finally, the underlying mechanisms of NLRP3 inflammasomes activation and caspase-1 signaling cascade were evaluated in human brain endothelial cell culture using NLRP3 gene silencing technique and dose-dependent effects of alcohol or CCs.

METHODS AND MATERIALS:

Reagents:

We purchased the antibodies to von Willibrand Factor (vWF), Caspase-1from Abcam (Cambridge, MA), antibody to NLRP3 from Lifespan Biosciences (Seattle, WA), antibody to IL-1 from Abgent (San Deigo, CA),and antibodies-actin and CD68 from Millipore (Billerica, MA).All secondary Alexa Fluor antibodies and Flou-3 were purchased from Invitrogen (Carlsbad, CA).Hematoxylin and Eosin were purchased from Surgipath (Richmond, IL). Cholesterol, Oil Red O, Propylene glycol, acetyl-L-carnitine (ALC), Atorvastatin (AVS),Lipopolysaccharides (LPS), and cytochalasin D (phagocytosis inhibitor) were purchased from Sigma-Aldrich (St. Louis, MO). The IL-1ELISA kit was from R&D Systems (Minneapolis, MN).The caspase inhibitor, z-YVAD-fmk was from Santa Cruz

Biotechnology (Santa Cruz, CA). Please see Table 1 for details of the antibodies source, catalogue numbers, and dilutions factors that were used for immunohistochemical staining and western blotting analyses.

Animals:

Five-week old male Sprague-Dawley rats were purchased from Charles River Laboratory (Wilmington, MA). Animals were maintained in sterile cages under pathogen-free conditions in accordance with institutional ethical guidelines for care of laboratory animals, National Institutes of Health guidelines, and the Institutional Animal Care Use Committee, University of Nebraska Medical Center. At week six, some animals underwent surgical implantation of catheters into the common carotid artery (CCA, procedure is described below). After complete wound healing, rats were acclimated to Lieber–DeCarli control or 29 % calorie (5% vol/vol) ethanol liquid-diets (Dyets Inc, Bethlehem, PA) with increments of 1%, 3% and 5% ethanol in a week. Rats were then pair-fed for 12 – 20 wks with liquid diets consisting of 1) normal control diet (ND), 2) High-fat diet (HD), 3) ethanol (EtOH), 4) ethanol+High-fat diet (EtOH(HD)), 5) ethanol+Highfat diet+ALC+AVS (EtOH(HD)+ALC +AVS), and 6)ALC+AVS alone in normal control diet. Pair feeding is based on daily liquid-diet consumption of alcohol. The macronutrient composition of liquid-diets as percent of total calories was control (47% carbohydrate, 35% fat, 18% protein) and ethanol (35% fat, 18% protein, 19% carbohydrate, 29% ethanol caloric intake). The daily alcohol consumption is translated to 0.7–1.0 g of ethanol/kg, considered heavy alcohol use compared to moderate alcohol users (0.3– 0.4 g of ethanol/kg). A J-shaped effect of alcohol in relation to cholesterol levels and mortality occurs only in moderate drinkers, since there is a linear increase of cholesterol levels and mortality rate in heavy chronic alcohol drinkers [27,28].

In separate experiments, 25% corn oil was added to ethanol-liquid diet containing 35 % fat making it a 60% high-fat diet (HD). High-fat diet was used to determine if obesity-like condition can worsen the levels of cholesterol, cholesterol crystals formation and atherosclerotic lesions in alcohol consumption. Combination of acetyl-L-carnitine (ALC) and Atorvastatin (AVS, Lipitor®) was used to determine its effectiveness in reducing oxidative damage, fat deposits, CCs formation and atherosclerosis. ALC/Lipitor® (2.0 mg/ml each) was mixed in the liquid-diets. We found that ALC/Lipitor® above 3.0 mg/ml caused skin rash and irritability in rats. Daily food consumption and weekly body weights were recorded. A minimum duration of 12 wks pair feeding was chosen because we could observe atherosclerotic lesions at this earliest time point. At week 13–14, non-surgery and surgery rats (10 animals/group) were subjected to functional experiments including immune cell infusion and MR imaging of atherosclerotic lesions. These animals were then sacrificed for neuropathological analyses. Animals were euthanized by ketamine/xylazine injection as approved by American Veterinary Medical Association Panel on Euthanasia. Blood samples were collected at the time of sacrifice to determine the levels of blood alcohol, cholesterol, CCs, neuronal specific enolase and S100 to correlate with pathological outcomes. Brain tissues were preserved in optimal cutting temperature compound (Tissue-Tek, Torrance CA) or fixed in 4% paraformaldehyde for histology. Brain tissue was also frozen for protein extractions and stored in −80°C until use.

Surgical procedures and intracranial blood pressure measurement:

Rats were anesthetized with ketamine-xylazine mixture (40–87 mg/kg of ketamine plus 5–13 mg/kg of xylazine) by i.p. injection. In our animal model of stroke, small size mouse pressure catheters were surgically implanted into the right common carotid artery (CCA) of rats to avoid obstruction of the cerebral blood flow. The first incision (site #1, 2–2.5 cm) was made on the right ventral side of the neck to expose CCA. The second incision (site #2, 2–3 cm) was made on the chest just below the xiphoid process, and a third incision (site #3, 2–2.5 cm) was made in the dorsal scapular region. A small hole (0.5 cm) was made just superior to the third incision as an outlet for the catheter. Using a stainless steel trochar, a subcutaneous tunnel was made from site #3 to #1 via site #2 external port for the catheter to run through the back of the animal just below the neck. Keeping this external port very short behind the neck avoided pulling out the catheters and achievement of 100% survival rate at post-surgery. We used 4.0 prolene suture to secure the implanted catheter to the internal muscles at sites #1, 2 and 3. All overlaying skins were sutured together using a simple interrupted suture technique with 4.0 prolene. All sutures were removed at 10–11 days post procedure. The step-by-step surgical procedure is shown in Figure 1 supplement. The tip of the catheter was capped with a stainless steel plug. This removable stainless steel plug is versatile for drug delivery, immune cell infusion and insertion of the intracranial blood pressure meter probe. The probe sensor attached to the intracranial blood pressure meter (ACQ 16, Data Science Instrument, St. Paul, MN) is equipped with a Pressure Control Unit (FP891B, Scisense Advancing Micro-sensor Technology, Ontario, Canada). Without restraining the animals or the use of anesthetic, we monitored the changes in diastolic and systolic intracranial blood pressure by using 1.2F pressure catheter from Scisense.

Analysis of cholesterol in serum:

The serum cholesterol levelswere determined by using cholesterol quantification assay kit from Abcam (Cat # ab65390), which provides a simple quantification of high-density-lipoprotein (HDL) and low-density lipoprotein (LDL or very low density LDL), after separation of HDL from LDL in serum samples. Briefly, cholesterol oxidase specifically binds to free cholesterol, which reacts with the probe to generate color at 570 nm and fluorescence at Ex/Em = 538/587 nm, while cholesterol esterase hydrolyzes cholesteryl ester into free cholesterol. Thus, cholesterol ester and free cholesterol can be detected separately in the presence and absence of cholesterol esterase in the reactions.

Analysis of cholesterol in brain tissue:

We analyzed the deposition of cholesterol in the brain vasculature and in deep brain tissue sections by Oil Red O staining and microscopy. Briefly, whole brain tissue sections (8 m thick) on glass slides were air dried for 40 min, fixed in ice-cold 10% formalin for 10 min, rinsed 3 times with distilled water and air dried for 10–15 min. Slides were immersed in absolute propylene glycol for 5 min and stained in pre-warmed (60°C) Oil Red O solution for 10 min; then embedded in 85% propylene glycol solution for 3 min, rinsed with distilled water, and then counter stained with hematoxylin for 1 min followed by rinsing in running tap water for 3 min and immersed in distilled water prior to mounting and overlaying in cover slips for microscopy analyses. Working solution of Oil Red O: Dissolve 0.005 g of Oil

Red O/mL absolute propylene glycol and heated to 95–100°C, filtered and stored at room temperature. We observed that Oil Red O staining was more versatile than the highly fluorescent cholesterol marker Filipin.

Detection of cholesterol crystals (CCs) in brain tissue:

We detected cholesterol crystals (CCs) in the brain tissue sections by Hematoxylene/Eosin staining technique and microscopy analysis. Briefly, whole brain cross sections containing microvessels (arterioles and capillaries) were air dried (5–10 minutes) and dehydrated by passing through series of 75, 95, 100 % ethanol and Xylene, each step having 2 dips for 3 min each. Tissue sections were gradually rehydrated in Xylene and reverse series of 100, 95, and 75 % ethanol followed by final immersion in distilled water for 5 min. Tissue sections stained in Hematoxylene (Surgipath, Harris formula) for 8 min were rinsed in running tap water for 20 min, immersed in $LiCO_3$ solution (1.36%) for 3 seconds, and then rinsed in tap water for 5 minutes. Tissues were then counter stained in Eosin (Surgipath) for 20 seconds, washed in distilled water and differentiated in acid-alcohol (1 % hydrochloric acid in 70% ethanol) solution for 30 seconds. Tissue sections were dehydrated in 95% and 100% ethanol with two dips for 3 min each, followed by two dips in Xylene (5 min each), air-dried, mounted in DPX mounting medium and then overlaid in cover slips for microscopy analyses.

Detection of CCs in blood samples:

We detected cholesterol crystals (CCs) in the whole blood cells by Giemsa staining (Sigma) technique and microscopy analysis. Briefly, 200 L of each blood sample was taken from all conditions that were assessed for serum cholesterol levels. The blood plasma samples were heated for 1 hour at 37°C. A well-mixed 10–20 L aliquot of each blood sample was transferred onto glass slide and gently smeared with a glass slide. The homogeneously distributed blood cells on the glass slides were fixed in methanol for 5–7 min, air-dried and stained with 6% Giemsa staining for 1 hour. Tissue slides were rinsed with buffer and air-dried. CCs were analyzed and quantified with a Leica DM 5500B microscope equipped with Leica DFC 450 cameras and Definiens tissue studio 3.6 software.

Bone marrow cell isolation, differentiation, and infusion of fluo-3 labeled cells:

Rat femur bones were removed immediately after euthanization under sterile conditions, washed in sterile PBS, and bone marrow were flushed out with fetal bovine serum (FBS) solution through the cut ends of the bones using 1ml syringe. Bone marrow suspension was filtered through a 40 m cell strainer and filtrate was centrifuged at 1800 rpm for 5 minutes at 4°C. Cell pellets were suspended in 1 ml of **medium A** [500ml DMEM F12, 50ml FBS, 500 l MCSF (macrophage colony–stimulating factor), 5ml fungizone, and 5ml penicillin/ streptomycin]. An aliquot of the cell suspension was dissociated by repeated trituration (10 times) to get the viable cell counts with Trypan Blue using Hemacytometer prior to culturing the cells in T-75 cm^2 flasks (2×10^6/flask) in medium A. Fresh media A was replaced every 48 hours. Fully differentiated macrophages were scrapped off on day 8, centrifuged at 1, 800 rpm for 5 min at 4°C, suspended in 1 ml FBS solution, labeled with 5 M Fluo-3 (Invitrogen), centrifugation washed off the unbound Fluo-3, and estimated the total number of cells.

Finally, 100 l of Fluo-3 labeled macrophage (2×10^6 cells) suspension in FBS was infused into the CCA via the implanted catheters using 30.5 G needle. Infiltrated Fluo-3 labeled macrophages around the perivascular or deep brain tissues were analyzed by confocal microscopy.

MRI imaging of BBB leakiness and atherosclerotic lesions assessment:

In order to establish the live imaging of atherosclerotic lesions and brain infarct volume, 14 – 15 weeks pair-fed surgery and non-surgery rats (10 animals/group) were subjected to functional assays such as Fluo-3 labeled immune cell infusion and magnetic resonance imaging. Atherosclerotic lesions/brain infarct volume was accessed by the function of gadolinium tracer ion permeability detected by MR imaging in Dr. Michael Boska's lab at UNMC. To validate this leakiness of the BBB, we also analyzed the leaking out of brain matter such as neuronal specific enolase (NSE) and astrocyte specific marker protein (S100β) in blood samples from all experimental animals. The presence of NSE (Alpha Diagnostic, Santa Monica, CA) and S100β (Abnova, Walnut, CA) in serum samples was analyzed by enzyme-linked immunosorbent assay (ELISA) following the respective manufacturer's instructions. This ELISA based detection of brain matter in blood samples is a reliable peripheral biomarker for BBB leakage and brain injury for neuropathological evidence. This is because degenerating neurons/astrocytes shed the cellular contents to the extracellular space, which are then leaked out into the blood stream via the leaky BBB.

Immunohistochemistry:

Brain tissue sections containing microvessels were washed with PBS, fixed in acetone-methanol (1:1 v/v) fixative, and then the tissue cellular antigen was blocked with 3% bovine serum albumin for 1 hr at room temperature in the presence of 0.4% Triton X-100 on glass slides. Tissue slides were incubated with respective primary antibodies overnight at 4°C. After washing off the respective primary antibodies, tissues were incubated with secondary antibody-Alexa fluor conjugate for 1 hr. Cover slips were mounted with immunomount containing DAPI (Invitrogen), and fluorescence microphotographs were captured by fluorescent microscopy (Eclipse TE2000-U, Nikon microscope, Melville, NY) using NIS elements (Nikon, Melville, NY) software.

HRP-DAB Immunohistochemistry:

Whole brain tissues fixed in 4% paraformaldehyde were cross-sectioned into 10 m thickness. Tissue slides were rinsed three times in TBS-T (12.10 g Tris + 17.52 g NaCl + 1600 mL distilled water +10 mL Tween 20, adjusted to pH 7.5 by hydrochloric acid), followed by blocking the tissues in 1% normal goat serum in phosphate buffer for 1 hour at room temperature. After applying 0.1% TritonX100 for 5 min and then flicking off the access, the tissue sections were incubated with primary antibody (Abcam) for overnight at 4°C using Invitrogen cover wells. The primary antibody was rinsed off three times with TBS-T, and the tissues were incubated with horseradish peroxidase (HRP) conjugated secondary antibody (Dako, Carpinteria, CA) for 45 min followed by three washes with TBS-T. Diluted 3,3'-diaminobenzidine (DAB) substrate chromagen was applied onto the tissues for 5–8 min to observe the color changes under dissecting microscope, followed by washing the tissue slides for 5 min under running tap water. Tissues were then counterstained with

already filtered Harris Hematoxylin for 2 min rinsed in running water 5 min, dipped in ammonia water for 10 seconds followed by three washes in running water. Dehydration of the tissue samples was done by progressively passing through the baths of 80%, 90%, 95%, 100% ethanol concentrations for 5 min each. Finally, three times washes with a hydrophobic Xylene removed the ethanol. Tissue slides were mounted with histomount and glass cover slips for microscopy analyses.

Cell culture and treatment:

Primary human brain endothelial cells (hBECs) obtained from Dr. Persidsky's Lab, Temple University School of Medicine were cultured as described previously[8,29]. Briefly, all cell culture plates and glass cover slips were pre-coated with type 1 rat-tail collagen (0.09 mg/mL in double distilled sterile water), aspirated the excess collagen and dried the plates overnight in sterile hood. Cell seeded onglass cover slips in 12-well plates (40,000 cells/well) were used for immunocytochemistry, while cells cultured in T 75 cm^2 flasks (1×10^6 cells/flask) were used for protein extractions. Cell culture media consisted of DMEM/F-12 containing 10 mM Hepes, 13 mM sodium bicarbonate (pH 7), 10% fetal bovine serum, penicillin and streptomycin (100 g/ml each, Invitrogen), which was changed with fresh media every 3 days until tight monolayers were formed in about 6–8 days. Fully confluent hBECs were treated with ethanol (50 mM) in the presence or absence of Lipitor (3 g/mL), ALC (100 M), caspase inhibitor z-YVAD-fmk (5 g/mL), cytochalsin D (2 M), LPS (1 g/mL) and cholesterol crystals (1 mg/mL), in DMEM/F-12 media containing 10 mM Hepes, 13 mM sodium bicarbonate (pH 7.0), 10% fetal bovine serum, penicillin and streptomycin (100 g/ml each, Invitrogen). Cholesterol crystals (CCs) were prepared by dissolving pure cholesterol in 95% ethanol (10 g/L) followed by heating at 60°C, filtered through Whatman filter paper to separate the CCs as previously described[30]. Large crystals were ground to 1–10 um size using a sterile mortar and pestle prior to exposure to hBECs cell culture. CCs were stored at −20°C for future use. Treated cells were incubated at 37°C for 24 hrs, then cell culture conditioned media were collected for analysis of secreted cytokine levels while the cells were washed with PBS prior to protein extraction for Western blot analysis. Cells cultured on glass cover slips were used for immunocytochemistry analysis.

NLRP3 siRNA transfection in hBECs:

Human brain endothelial cells (hBECs) were seeded on rat tail collagen coated 6-well plates (2×10^5 cells/well) in DMEM/F-12 media containing HEPES (10 mM), sodium bicarbonate (13 mM, pH 7), 10% fetal bovine serum, penicillin and streptomycin (100 g/ml each, Invitrogen). After 24 hours (60–80% confluent of cells), the cells were transfected with siRNA (5 nM per well) targeted at NLRP3 mRNA (Hs_CIAS1_9; Cat No. SI02634030; Qiagen, Valencia, CA) or with AllStars Negative Control siRNA (5 nM per well; Qiagen), using the HiPerFect transfection reagent (Cat. No. 301704; Qiagen) according to the manufacturer's instructions. After 24 hr of incubation with the siRNAs with or without EtOH (50 mM) and cholesterol crystals (1 mg/mL), the cells were washed with PBS and incubated for a further 12 h in serum-free culture medium. Finally, the cells were harvested, protein was extracted and the expression was analyzed by Western blotting.

Immunocytochemistry:

Cells cultured on glass cover slips were washed with PBS, fixed in acetone-methanol (1:1 v/v) fixative, blocked the cellular antigen with 3% bovine serum albumin at room temperature for 1 hr in the presence of 0.4% Triton X-100 and incubated with respective primary antibodies such as mouse anti-NLRP3 (1:250 dilution), rabbit anti-von Willebrand factor (vWF) (1:150 dilution) and rabbit anti-caspase-1 (1:500 dilution) overnight at 4°C. After washing with PBS, cells were incubated for 1 hr with secondary antibody: anti-mouse-IgG Alexa fluor 488 for NLRP3; anti-rabbit-IgG Alexa fluor 594 for vWF; anti-rabbit-IgG Alexa fluor 488 for caspase-1. Cover slips were then mounted onto glass slides with immunomount containing DAPI (Invitrogen), and fluorescence microphotographs were captured by fluorescent microscopy (Eclipse TE2000-U, Nikon microscope, Melville, NY) using NIS elements (Nikon, Melville, NY) software.

Analysis of IL-1levels by ELISA assay kit:

The changes in the levels of IL-1in the culture media and blood samples from animal studies were analyzed bycommercially available enzyme-linked immunosorbent assay (ELISA) kit from R&D Systems, (Minneapolis, MN) as per manufacturer's instructions.

Western blotting:

The hBECs cultured in T-75 cm^2 flasks were lysed with CellLytic-M (Sigma) at 4°C. Then cell lysates orbrain tissuehomogenates from animal studies were centrifuged at 14000 × gat 4°C, and then total protein concentrations in respective samples were estimated by BCA (Thermo Scientific, Rockford, IL). We loaded 20 g protein/lane and resolved the various molecular weight proteins by SDS-PAGE on gradient gels (Thermo Scientific) and then transferred the protein onto nitrocellulose membranes. After blocking, membranes were incubated for overnight with primary antibody such as mouse anti-NLRP3 (1:1000), rabbit-anti-caspase-1 (1:2000) and rabbit anti-IL-1 (1:250) at 4°C followed by 1 hr incubation with horse-radish peroxidase conjugated secondary antibodies. Immunoreactive bands were detected by West Pico chemiluminescence substrate (Thermo Scientific). Data were quantified as arbitrary densitometry intensity units using the Gelpro32 software package (Version 3.1, Media Cybernetics, Marlow, UK).

Statistical Analysis:

GraphPad Prism V5 software (Sorrento Valley, CA) was used for all statistical analysis.Data in graphs are shown as means ±SEM; N = X. In the present studies, wherever the numeric values of N are indicated, it represents the actual number of animals/samples used for that specific experiments or the actual number of experiments performed in cell culture setting, and not the number of replicates per experimental condition.Comparisons between samples were performed by one-way ANOVA with Bonferroni post-hoc tests. Differences between groups with $p < 0.05$ were considered significant.

RESULTS

Adhesion and infiltration of immune cell into the brain.

Alcohol promotes immune cell adhesion and infiltration into the brain via the oxidatively injured sites of the capillary [9,22]. To examine cell proliferation at this site of injury in the arteriole/capillary walls, we first infused Fluo-3 labeled macrophages (2 million cells/rat)through the rat common carotid artery catheter implantation those have been pair-fed for 12 weeks. Animals were euthanized at 2 hrs after cell infusion. Cell infiltration across thearterial/capillary vessels (the blood-brain barrier, BBB) at different segments was analyzed in surgically removed intact arterioles (Fig 1A-B) and in the brain tissue cross sections containing capillaries (Fig 1C-D). Infiltration of labeled cells (indicated by macrophage marker CD68) in basolateral side (brain side) of the capillary was highly localized at the injury sites of the capillary endothelium marker von Willebrand factor (vWF) in ethanol (EtOH) or EtOH high-fat (HD) compared with control (Fig 1C-D). Cholesterol layering appeared to promote immune cell infiltration because normalization of blood cholesterol levels by ALC+AVS administrationsignificantly prevented the induction of EtOH/EtOH(HD) mediated cell infiltration into the brain (Fig 1A-D).

The mean of total cholesterol levels expressed in mg/dL were 15820 for normal control diet (ND), 22015 for high fat diet (HD), 25518 for EtOH, 26410 for EtOH(HD) and 16618 for EtOH(HD)+ALC+AVS. The serum high-density-lipoprotein (HDL) levels(Fig 2A)were expressed as the ratio of the total cholesterol. We observed that ethanol or ethanol high-fat diet consumptionsignificantly lowered the serum HDL levels, but not HD alone compared with controls (Fig 2B). Similarly, the serum low-density lipoprotein (LDL) levels(Fig 2C) were expressed as the ratio of HDL. Ethanol diet, ethanol high-fat diet, or HD alone consumptionelevated the levels ofvery low density LDL in serum, which was significantly abrogated by the combined therapy of acetyl-Lcarnitine and Atorvastatin (ALC/Lipitor®) (Fig 2D). Interestingly, the high-fat diet did not further increase the serum LDL levels in EtOH group. It is possible that activation of cholesterol synthesizing enzyme HMG-CoA reductase by ethanol increased the *de novo* synthesis of cholesterol, the high-fat diet alone may not significantly contribute to this biosynthesis.

We also examined the deposition of cholesterol inside the deep brain tissue of the frontal cortex byOil red O staining and microscopy analyses as well as quantified the levels of cholesterol deposit by using ImageJ software. The positive staining of cholesterol deposit in the frontal cortex was observed only in the presence of alcohol (Fig 2E-F). These data suggest that alcohol consumption and high-fat diet consumption could be potential risk factors for tilting the ratio of HDL to LDL in the circulation and promote a *de novo* synthesis of cholesterol in the brain. Administration of ALC/Lipitor®effectively restores HDL/LDL physiological imbalance caused by chronic alcohol consumption and obesity-like condition.

Deposition of cholesterol causes thickening of vessel walls:

Alcohol mediated elevation of cholesterol in the circulation and immune cell invasioninto the endothelium is expected to build-up lipid bodies in the lumen of vasculature as an early

event of atherosclerosis. Thus, we next analyzed the deposition of cholesterol and thickening of vessel walls in different segments of brain microvessels. Ethanol or EtOH(HD) diet ingested animals showed a marked cholesterol deposit and perivascular thickening of artery (Fig 3A a-e), arteriole (Fig 3B f-j), and capillary (Fig 3C k-o)in high-fat diet (HD), ethanol (EtOH), and EtOH(HD), compared with EtOH(HD)+ALC+AVS or controls. The accumulation of cholesterol is more pronounced in the capillary, which was likely to result from the occlusion of cholesterol at the capillary bed.Since thevessel diameterbecomes narroweralong the arterial,arteriole, and capillarysegments, the deposition of cholesterol is expected to be more packed in the capillary.The vessel walls' thickness was about 2–4 μm in experimental conditions and about 1–2 μm in controls. Lipitor® and ALC prevented the alcohol-induced cholesterol deposit and thickening of the vessel walls.

Lowering of cholesterol prevents formation of cholesterol crystals and hypertension during alcohol consumption.

To the best of our knowledge, this is the first report to indicate that elevated levels of cholesterol in alcohol consumption is converted to sharp edges of cholesterol crystals (CCs). We observed that cholesterol deposits on the luminal walls of the cerebral vasculature become crystallized in an alcohol environment. Crystallization of cholesterol appears to occur only in the presence of alcohol because CCs were not formed in high-fat dietwithout alcohol in spite of a huge cholesterol accumulation in the vasculature (Fig 4A). We noted that lowering of cholesterol levels by ALC/AVS (observed in Figs 2 and 3) prevented the formation of CCs in EtOH(HD)consumption. This fact indicate the importance of the threshold levels of cholesterol and ethanol for the formation of CCs in physiological conditions, which is addressed in supplementary figure 6 C and in the discussion section.

We also evaluated the idea that normalization of blood cholesterol levels and prevention of CCs formation by ALC+AVS is expected to normalize blood pressure. Thus, we monitored the cardiovascular and intracranial blood pressure by Scisense blood pressure meter probe in our experimental conditions at 14 weeks of pair feeding paradigms. Administration of ALC +AVSat the *onset* of EtOH or EtOH(HD) consumption significantly normalized the EtOH/ EtOH(HD)induced cardiovascular and intracranial arterial blood pressure to control levels (Fig. 4B-C).The monitoring of cardiovascular or the intracranial blood pressure was achieved by inserting the catheter pressure sensor either towards the aorta or towards the brain side from the site of catheter probe implantation.The average diastolic and systolic cardiovascular blood pressures were 80 5 and 122 4 mmHg for controls, 90 6 and 144 5mmHg for high-fat diet, HD, 92 4 and 150 6mmHg for EtOH, 96 4 and 158 7 mmHg for EtOH(HD), and 83 5 and 126 5 mmHg for EtOH(HD)+ALC+AVS. The increase in blood pressures in HD, EtOH, or EtOH(HD) diet ingested groups were significantly higher ($p < 0.02$) than the control or the EtOH(HD)+ALC+AVS condition.

Detection of neuropathy and BBB leakage around the atherosclerotic lesions.

The prevention of CCs formation and hypertension by ALC+AVS would be expected to diminish cerebral atherosclerotic lesions. But those alcohol-ingesting animals with positively detected CCs would be expected to exhibit the piercing of the capillary walls by the sharp edges of CCs with associated bulging of atherosclerotic lesions. This cause and effect of

CCs was clearly indicated by the bulging of atherosclerotic lesions, which were significantly protected by ALC+AVS administration(see arrows and inset in suppl. Fig 2A). To drive the point that cerebral vascular injury initiates inflammation and neuronal degeneration, we observed a distinct neuropathy specifically localized around the perivascular region as indicated by increased tau-phosphorylation in chronic alcohol consumption (suppl. Fig 2B). Such atherosclerotic lesions in the arteriole/capillary endothelium promote the infiltration of immune cells into the brain as well as leaking out of degenerated brain matter across the leaky blood-brain barrier (BBB). The magnetic resonance brain imaging with gadolinium tracer ion confirmed the leakage of BBB and brain infarct volume in alcohol ingested animals, but significantly protected by ALC+AVS administration (Fig 5A). In parallel with these pathologic outcomes, we found elevated levels of brain matter such as S100 (Fig 5B) and neuronal specific enolase (NSE, Fig 5C) in serum samples from alcohol-ingesting animals. It is likely that NSE may be leaking out from the degenerating tauopathy (degenerated neurons) and S100 from the dislodged astrocyte end feet in the perivascular region. A combined therapy of ALC+AVS was also found to protect the leakiness of the BBB, and leakage of NSE or S100β into the circulation (Fig 5A-C).

Clinical validation of animal model observations in alcohol users.

We then wanted toestablish if CC formation observed in our animal model of alcohol consumption would be relevant to human alcohol users. To validate the clinical relevance, we first examined human brain tissue sections in alcohol users for the presence of CCs, but failed to observe CCs in these samples. Inability to detect CCs in these tissue samples was attributed to limited brain tissue samples' size (30–40mg) where arterioles/capillaries were absent. Next, we examined the presence or absence of CCs in blood samples from subjects with alcohol dependence and control subjects matched on the basis of age, smoking habits and gender. Table 2 shows the total number of subjects enrolled and the detailsof clinical information. De-identified whole blood samples or lyzed blood samples from alcohol users and control subjects were procured from Dr. Burnham, University of Colorado Hospital, Aurora, Colorado (UNMC IRB#29912-NH). Together with human blood samples, we also analyzed the presence of CCs in blood samples from our animal studies. Giemsa staining and microscopy analysis (see methods) detected the presence of CCs in intact whole blood samples from alcohol consumed animals only (Fig 6A). Surprisingly, we also detected CCs in intact whole blood samples (Fig 6B, second panel) and in - 80°C lyzed frozen blood samples (Fig 6B, fourth panel) from alcohol users, but not innon-alcohol user subjects (Fig 6B, first and third panel). Distinct CCs were seen in between the intact blood cells whereas clusters of CCs were observed in - 80°C frozen blood samples. CCs appeared to form clusters of long branching aggregates in the absence of intact cell body barriers. The clusters of CC aggregates were similar to sulfonamide crystals commonly found in the urine of patients under sulfonamide drug medication. We confirmed that these alcohol user subjects were not on sulfonamide drug treatment at the time of blood sampling.

Threshold of CCs formation with varying concentrations of cholesterol and ethanol.

In addition to the preventive effects of ALC/Lipitor®, we gained significant knowledge on the kinetic profile of CCs formation in response to dose-, time-, and temperature-dependent effects of alcohol or cholesterol. The threshold of CC formation was determined by

incubating 0.25 – 4.0 mg of cholesterol for 1 – 4 hours in buffer or whole blood from control animals in the presence of 0.5 – 2 % of ethanol at 37°C, 40°C and 50°C. Formation of CCs increased with increase in cholesterol levels, alcohol concentrations and temperature. The lowest threshold of CCs formation in a well-controlled experiment was found to be at 0.5 mg of cholesterol in 1% of ethanol incubated for 2 hours at 37° (Fig 6C). The threshold in blood samples was found to be 0.8 mg cholesterol level in the same experimental protocol. Since the upper limit of plasma cholesterol level in normal healthy subjects is 1.0 mg/mL, a risk of CCs formation exists in healthy subjects with plasma cholesterol levels of 0.8 – 1.0 mg/mL, even if alcohol is used only occasionally.

Formation of cholesterol crystals activates NLRP3 inflammasome in alcohol intake.

Cholesterol crystals have been shown to activate NLRP3 inflammasome, an authentic marker for atherosclerosis. Since we demonstrated here the presence of CCs and atherosclerotic lesions, we then examined the profile of NLRP3 inflammasomes and its downstream caspase-1 activation in brain tissue sections from controls, EtOH, EtOH +ALC/AVS liquid diets ingested animals as well as in brain tissue sections from acute infusion of cholesterol or CCs rats. We found high level expression of NLRP3 inflammasome and subsequent activation of caspase-1 in EtOH diets (Fig 7A g & j) that were validated by significant increase in respective protein levels (Fig 7B), specifically in the brain capillaries. Similarly, acute infusion of cholesterol (chol) or CCs (CholCryst) elevated the levels of NLRP3 and caspase-1 protein in brain microvessels compared with control (Fig 7B). Interestingly, chronic alcohol intake or acute CCs infusion induced the expression and protein levels of NLRP3 inflammasomes and caspase-1 expression (suppl.Fig 3A)and protein contents (suppl.Fig 3B)in the brain cortical region. Taken together, these data indicate that alcohol intake can activate the atherosclerotic marker NLRP3/caspase-1 via CCs formation, and that ALC/AVS can prevent the activation by abrogating CCs formation.

Understanding the molecular mechanisms of caspase-1 activation via NLRP3 inflammasome signaling in alcohol exposure.

It is obvious that formation of CCs in alcohol intake increases the level of NLRP3 inflammasome, particularly in the brain capillaries. We then examined the underlying mechanisms of caspase-1 activation mediated by NLRP3 inflammasomes signaling in human brain endothelial cell (hBECs), the primary cell component of the BBB in brain capillary. We first determined the dose-dependent effects of ethanol or CC on NLRP3 expression andIL-1release in hBECs culture in the presence or absence of a positive control lipopolysaccharide (LPS). The release of IL-1 was used as an indicator for caspase-1 activation. Our data revealed that alcohol (suppl.Fig 4A)or cholesterol crystal(suppl.Fig 4B)dose-dependently induced NLRP3 inflammasome either in the absence or presence of LPS. In agreement with NLRP3 inflammasome induction, both alcohol (suppl.Fig 4C)and cholesterol crystal(suppl.Fig 4D)dose-dependentlyincreased the release of IL-1in hBECs cultured media with/without LPS.

We then treated hBECs culture with optimal concentration of ethanol or CCs (CholCryst) in the presence or absence of ALC/AVS to examine the changes in the levels of NLRP3

inflammasomes and caspase-1 protein expression. ALC/AVS was included in the ethanol condition to mimick our animal model experimental setting. As expected, 50 mM of EtOH or 1 mg/ml of CCs simultaneously increased the levels of NLRP3 and caspase-1 expression that were diminished by the presence of ALC/AVSas indicated by immunofluorescene confocal imaging (Fig 8A a-i).Notice that CCs particles were taken up by hBECs (see arrows). However, CCs remained extracellular in the presence of phagocytosis inhibitor Cytochalasin-D (data not shown), suggesting that uptake/binding of CCs to cell is prerequisite for activation of cytosolic NLRP3 inflammasomes. Changes in NLRP3 inflammasomes or caspase-1 expression were further validated by Western blotanalyses of the actual protein levels, where we also delineated the signaling mechanism by using respective inhibitors zYVAD-fmk/CDor a positive control LPS. Figure 8B showed that EtOH-induced upregulation of NLRP3 inflammasomes protein levels were decreased by phagocytosisinhibitor Cytochalasin-D (CD) or by ALC/AVS. Similarly, the increase in pro-caspase-1 and caspase-1 levels by EtOH was significantly diminished by caspase-1 inhibitor zYVAD-fmk (5 g/ml), CD, or ALC/AVS respectively compared with controls (Fig 8C).As expected, treatment of hBECs with CCs significantly increased the levels of NLRP3 inflammasomes and procaspase-1/caspase-1 compared with control. In the same experimental setting, we also determined the IL-1βlevels by Western blotting in hBECs cultured mediaand in cell lysates as a functional read-out indicator of caspase-1 activation. In agreement with caspase-1 activation, we found that both EtOH and CCs respectively elevated the levels of IL-1in cell culture supernatants and cell lysates, where abrogated by zYVAD-fmk or CD (Suppl. Fig 5).

Dose-dependent effects of ethanol or CCs on IL-1 levels in hBECs.

Since activation of caspase-1 leads to maturation of IL-1β, we next analyzed the secreted and endogenous levels of IL-1β in hBECs following exposure to different concentrations of EtOH or CCs in the presence or absence of the inhibitor zYVAD-fmk or CD. Figure 9 A and B showed the dose-dependent elevation of IL-1secretion in cell culture supernatants after hBECs exposure to different concentrations of EtOH or CCs for 24 hours as determined by ELISA kit. Similarly, EtOH or CCsdose-dependently increased the endogenous levels of IL1in the cell lysates determined by Western blotting(Fig 9 C and D). The EtOH/CC-induced levels of IL-1 in secreted or endogenousform in hBECs were suppressed by zYVAD-fmk or CD.

NLRP3 inflammasome mediated activation of caspase-1 increases IL-1β levels in the circulation, brain arterial vessels, and in cortical brain region.

To complement the *in vitro* results, we examined the changes of IL-1 levels in blood samples, brain arterial vessels, and in cortical brain tissuesamples from chronic alcohol consumption and acute cholesterol crystal infusion. We found that alcohol consumption or CCs infusion showed a significant 3–4 fold increments of IL-1βlevels in blood serum ELISA analysis(suppl.Fig 6A), in brain arterial vessels(suppl.Fig 6B), or in brain tissue samples Western blot analyses (suppl.Fig 6C) compared with respective controls. These observations were in agreement with the *in vitro* findings that showed 3–4 fold elevated levels of IL-1in hBECs when exposed to EtOH/CCs or to LPS compared with untreated controls. These data validate the point that CC-mediated activation of NLRP3

inflammasome and downstream caspase-1 activation triggered theelevation andmaturation of IL-1 levels in chronic alcohol consumption.

NLRP3 inflammasome gene silencing investigation.

To understand the molecular signaling mechanisms downstream to NLRP3, we performed NLRP3 gene silencing of hBECs in alcohol/CCs exposure condition (see method section for hBECs transfectionof hBECs with siRNA). Briefly, NLRP3 siRNA hBECs or scrambled siRNA hBECs culture were exposed to EtOH or CCs for 24 hours. Then we examined the changes in the levels of NLRP3, Caspase-1 and IL-1 in cell lysates or supernatants by Western blotting and ELISA using -actin as internal control. We observed that silencing the NLRP3 inflammasome gene in hBECs significantly attenuated the alcohol/CC-induced protein levels of NLRP3, caspase-1 and IL-1in cell lysates compared with control or scrambled siRNA as shown byrepresentativeimmunoreactive bands (Fig 9 E) and quantification of the respective immunoreactive bands to that of -actin (Fig 9 F). The activation of caspase-1 by alcohol/CCand abrogationof caspase-1 by NLRP3 siRNA in hBECs were also confirmed by the levels ofIL-1βrelease in cell culture supernatants compared with control or scrambled siRNA(Fig 9 G). The results suggest that activation of NLRP3 inflammasome is not only an authentic marker for atherosclerosis, but also a promoter of neuroinflamation through the production of downstream proinflammatory cytokine IL-1β release.

DISCUSSION

We demonstrated here for the first time that alcohol promotes formation of cholesterol crystals (CCs) and induction of atherosclerotic lesions. The high-fat diet alonedid not form CCs in the absence of alcohol even though there was elevation of cholesterol levels. Therefore, we focused our discussion and data interpretation on the CC-elicited development of atherosclerosis through NLRP3 inflammasome signaling pathway involving the activation of caspase-1 and regulation of secreted/intracellular IL-1β.It may be noted here that the comparison of the animal age-related factor is certainly not relevant to the clinical outcome of stroke incidence in older-adult patient. This is because the age of the rats were 22 – 29 weeks old at the time of sacrifice, which is approximately 18 – 19 years of human age. The most important factors are the elevation of cholesterol levels and formation of cholesterol crystals in the presence of alcohol for the induction of cerebral atherosclerotic lesions, irrespective of age.

The therapeutic prevention of the immune cell adhesion/infiltration at the site of capillary oxidative injury, the cholesterol deposition and crystallization,and atherosclerosis was carried out in our animal model of chronic alcohol consumption[22].Whereas, we examined the underlying molecular signaling mechanisms of NLRP3 inflammasome activation by alcohol/CCs and regulation of the downstream caspase-1/IL-1β release in hBECs culture using NLRP3 gene silencing techniques. Our findings showed that lowering of cholesterol levels by ALC+AVS concomitantly prevented cell invasion in the vasculature, thereby minimizing the early event of atherosclerosis. This was supported by reduction of serum cholesterol levels, cholesterol build-up in different size of the vessels, thickening of arterial/

capillary walls, and intracranial blood pressure in alcohol consumptionfollowing ALC/Lipitor® administration.The increase in serum LDL cholesterol levels associated with alcohol diet ingested animals in this study is similar to serum LDL cholesterol levels observed in human alcoholics[31,32].

Using the animal model of CCs embolization, it has been shown that microinjection of CCs into the internal carotid artery disrupts the BBB and cognitive function[33,34]. To date, there is no evidence of CCs formation in animal model or human studies arising from alcohol consumption. Thus, observation of CCs formation in the present studiesbridged a significant knowledge gap discovery in uncovering the mechanisms of atherosclerosis. One obvious question is to address the solubility of CCs or cholesterol in physiological condition. We verified that CCs and cholesterol readily dissolve in absolute ethanol as reported previously [35]. We found that solubility of CCs/cholesterol increases from 70% to 100% of ethanol, but will not dissolve in ethanol less than 60% (v/v) at room temperature. This observation was significant and clinically relevant because blood alcohol levels of >60% (v/v) would likely be lethal to humans. Importantly, alcohol related poikilothermic effects, a characteristic rise and fall of body temperature in alcoholism [36] may impact CCs formation in real life. For example, hyperthermia commonly observed in alcohol withdrawal in humans with chronic heavy alcohol consumption may promote cholesterol solubility, whereas subsequent hypothermia when withdrawal has subsided may crystallize cholesterol. We found that lower threshold of CCs formation in blood samples was0.8 mg cholesterol in 1% of ethanol incubated for 2 hours at 37°, which was slightly higher than the lower threshold (0.5 mg cholesterol) in a well-controlled cholesterol crystallization in acetone (see Fig 6 C). Establishment of this threshold is clinically significant because it suggests a much greater risk of CCs formation and development of atherosclerosis in high cholesterol subjects even if alcohol is used occasionally.

We administered ALC/Lipitor® at the *onset* of ethanol liquid diet feeding in order to prevent the occurrence of alcohol-induced oxidative damage, cholesterol elevation, CCs formation, and atherosclerosis. Administration of ALC/Lipitor®was also expected to normalizethe blood pressure from alcohol-induced elevation of cholesterol as observed in figure 3, and we found that ALC/Lipitor® lowered both the cardiovascular and intracerebral blood pressures (see Figure 4). After 12 weeks of ethanol diet ingestion, ALC/Lipitor® is unlikely to reverse this intracranial hypertension because by then there would have been an abundant bioavailability of CCs that cannot be cleared or dissolved by ALC/Lipitor®. Thus, a biological solvent that can accelerate the dissolving of CCs in conjunction with lowering the blood cholesterol levels may represent an opportunity to improve cerebrovascular health in this at-risk population. Recent discovery of β-cyclodextrin conjugated superparamagnetic nanoparticles [37] that selectively bind to CCs will be a vital diagnostic tool for imaging of CCs in CC-related neurological diseases such as atherosclerosis. Importantly, our observation of CC formation in animal model of atherosclerosis was validated in the alcohol environment in human subjects, which has a significant clinical relevance to the health of chronic alcohol consumers.

We showed here that formation of CCs in alcohol consumption either in normal or high-fat diet ingestion activated NLRP3 inflammasomes in brain capillary endothelium, which in

turn regulated the downstream activation of caspase-1 and IL-1release as amolecular signaling mechanism. Maturation and secretion of a pro-atherogenic cytokinesuch as IL-1enhanced the recruitment and infiltration of immune cells at arterial inflammatory site as demonstrated in the present studies. Promotion of arterial wallinflammation and development of atherosclerosis by myriad of cytokines have been shown in the severity of coronary arterial disease [38,39]. By using specific inhibitors such as zYVAD-fmk, CD or different concentrations of CCs/ethanol, we also validated ourhypothesis that activation of NLRP3 in alcohol consumption triggered the caspase-1 mediated IL-1 regulation. Our hypothesized underlying mechanisms is supported by strong correlation between caspase-1 activation and IL-1 levels in secreted/endogenous form from both the *in vivo* and *in vitro* analyses (see Figure 9 and Suppl. Fig 6). The abrogationof alcohol/CC mediated activation of caspase-1 and IL-1βrelease resulting from NLRP3 inflammasome was confirmed by silencing of NLRP3 gene in human brain endothelial cell culture.

In conclusion, accumulation and crystallization of cholesterol in brain capillary oxidative injury sites triggered the activation of NLRP3/caspase-1 and early development of cerebral atherosclerosis in chronically high alcohol users. Uncovering the molecularmechanisms of this disease progression has streamlined a preventive step for health benefits, which is the long-term goal of ongoing research in clinical studies. This new knowledge on the causative and preventive mechanism of this significant disease in alcohol abuse is expected to have broad implications in preventing the silent killer, stroke.

Supplementary Material

Refer to Web version on PubMed Central for supplementary material.

ACKNOWLEDGEMENTS

This work was supported by grant 1R21AA022734-01A1,R21 AA020370-01A1 (to JH) and R24 AA019661 (to ELB).

REFERENCES

1. Donnan GA, Fisher M, Macleod M, Davis SM (2008) Stroke. Lancet 371: 1612–1623. [PubMed: 18468545]
2. Jerrard-Dunne P, Sitzer M, Risley P, Steckel DA, Buehler A, et al. (2003) Interleukin-6 promoter polymorphism modulates the effects of heavy alcohol consumption on early carotid artery atherosclerosis: the Carotid Atherosclerosis Progression Study (CAPS). Stroke 34: 402–407. [PubMed: 12574550]
3. Kiechl S, Willeit J, Rungger G, Egger G, Oberhollenzer F, et al. (1998) Alcohol consumption and atherosclerosis: what is the relation? Prospective results from the Bruneck Study. Stroke 29: 900–907. [PubMed: 9596232]
4. Mostofsky E, Burger MR, Schlaug G, Mukamal KJ, Rosamond WD, et al. (2010) Alcohol and acute ischemic stroke onset: the stroke onset study. Stroke 41: 1845–1849. [PubMed: 20634479]
5. Patra J, Taylor B, Irving H, Roerecke M, Baliunas D, et al. (2010) Alcohol consumption and the risk of morbidity and mortality for different stroke types-a systematic review and meta-analysis. BMC Public Health 10: 258. [PubMed: 20482788]
6. Haorah J, Ramirez SH, Schall K, Smith D, Pandya R, et al. (2007) Oxidative stress activates protein tyrosine kinase and matrix metalloproteinases leading to blood-brain barrier dysfunction. J Neurochem 101: 566–576. [PubMed: 17250680]

7. Haorah J, Ramirez SH, Floreani N, Gorantla S, Morsey B, et al. (2008) Mechanism of alcohol-induced oxidative stress and neuronal injury. Free Radic Biol Med 45: 1542–1550. [PubMed: 18845238]
8. Haorah J, Knipe B, Gorantla S, Zheng J, Persidsky Y (2007) Alcohol-induced blood-brain barrier dysfunction is mediated via inositol 1,4,5-triphosphate receptor (IP3R)-gated intracellular calcium release. J Neurochem 100: 324–336. [PubMed: 17241155]
9. Abdul Muneer PM, Alikunju S, Szlachetka AM, Haorah J (2012) The mechanisms of cerebral vascular dysfunction and neuroinflammation by MMPmediated degradation of VEGFR-2 in alcohol ingestion. Arterioscler Thromb Vasc Biol 32: 1167–1177. [PubMed: 22402362]
10. Rump TJ, Abdul Muneer PM, Szlachetka AM, Lamb A, Haorei C, et al. (2010) Acetyl-L-carnitine protects neuronal function from alcohol-induced oxidative damage in the brain. Free Radic Biol Med 49: 1494–1504. [PubMed: 20708681]
11. Haorah J, Floreani NA, Knipe B, Persidsky Y (2011) Stabilization of superoxide dismutase by acetyl-l-carnitine in human brain endothelium during alcohol exposure: novel protective approach. Free Radic Biol Med 51: 1601–1609. [PubMed: 21782933]
12. LaPorte R, Valvo-Gerard L, Kuller L, Dai W, Bates M, et al. (1981) The relationship between alcohol consumption, liver enzymes and high-density lipoprotein cholesterol. Circulation 64: III 67–72.
13. Sane T, Nikkila EA, Taskinen MR, Valimaki M, Ylikahri R (1984) Accelerated turnover of very low density lipoprotein triglycerides in chronic alcohol users. A possible mechanism for the up-regulation of high density lipoprotein by ethanol. Atherosclerosis 53: 185–193. [PubMed: 6517974]
14. Floreani NA, Rump TJ, Abdul Muneer PM, Alikunju S, Morsey BM, et al. (2010) Alcohol-induced interactive phosphorylation of Src and toll-like receptor regulates the secretion of inflammatory mediators by human astrocytes. J Neuroimmune Pharmacol 5: 533–545. [PubMed: 20379791]
15. Galkina E, Ley K (2009) Immune and inflammatory mechanisms of atherosclerosis (*). Annu Rev Immunol 27: 165–197. [PubMed: 19302038]
16. Duewell P, Kono H, Rayner KJ, Sirois CM, Vladimer G, et al. (2010) NLRP3 inflammasomes are required for atherogenesis and activated by cholesterol crystals. Nature 464: 1357–1361. [PubMed: 20428172]
17. Freigang S, Ampenberger F, Spohn G, Heer S, Shamshiev AT, et al. (2011) Nrf2 is essential for cholesterol crystal-induced inflammasome activation and exacerbation of atherosclerosis. Eur J Immunol 41: 2040–2051. [PubMed: 21484785]
18. Tschopp J, Schroder K (2010) NLRP3 inflammasome activation: The convergence of multiple signalling pathways on ROS production? Nat Rev Immunol 10: 210–215. [PubMed: 20168318]
19. Martinon F, Mayor A, Tschopp J (2009) The inflammasomes: guardians of the body. Annu Rev Immunol 27: 229–265. [PubMed: 19302040]
20. Martinon F, Burns K, Tschopp J (2002) The inflammasome: a molecular platform triggering activation of inflammatory caspases and processing of proIL-beta. Mol Cell 10: 417–426. [PubMed: 12191486]
21. Thornberry NA, Bull HG, Calaycay JR, Chapman KT, Howard AD, et al. (1992) A novel heterodimeric cysteine protease is required for interleukin-1 beta processing in monocytes. Nature 356: 768–774. [PubMed: 1574116]
22. Alikunju S, Abdul Muneer PM, Zhang Y, Szlachetka AM, Haorah J (2011) The inflammatory footprints of alcohol-induced oxidative damage in neurovascular components. Brain Behav Immun 25 Suppl 1: S129–136. [PubMed: 21262340]
23. Durukan A, Tatlisumak T (2009) Ischemic stroke in mice and rats. Methods Mol Biol 573: 95–114. [PubMed: 19763924]
24. Pettegrew JW, Levine J, McClure RJ (2000) Acetyl-L-carnitine physical-chemical, metabolic, and therapeutic properties: relevance for its mode of action in Alzheimer's disease and geriatric depression. Mol Psychiatry 5: 616–632. [PubMed: 11126392]
25. Puato M, Faggin E, Rattazzi M, Zambon A, Cipollone F, et al. (2010) Atorvastatin reduces macrophage accumulation in atherosclerotic plaques: a comparison of a nonstatin-based regimen in patients undergoing carotid endarterectomy. Stroke 41: 1163–1168. [PubMed: 20413736]

26. Amarenco P, Goldstein LB, Sillesen H, Benavente O, Zweifler RM, et al. (2010) Coronary heart disease risk in patients with stroke or transient ischemic attack and no known coronary heart disease: findings from the Stroke Prevention by Aggressive Reduction in Cholesterol Levels (SPARCL) trial. Stroke 41: 426–430. [PubMed: 20110538]
27. Plunk AD, Syed-Mohammed H, Cavazos-Rehg P, Bierut LJ, Grucza RA (2014) Alcohol consumption, heavy drinking, and mortality: rethinking the j-shaped curve. Alcohol Clin Exp Res 38: 471–478. [PubMed: 24033586]
28. Pitsavos C, Makrilakis K, Panagiotakos DB, Chrysohoou C, Ioannidis I, et al. (2005) The J-shape effect of alcohol intake on the risk of developing acute coronary syndromes in diabetic subjects: the CARDIO2000 II Study. Diabet Med 22: 243–248. [PubMed: 15717869]
29. Abdul Muneer PM, Alikunju S, Szlachetka AM, Murrin LC, Haorah J (2011) Impairment of brain endothelial glucose transporter by methamphetamine causes blood-brain barrier dysfunction. Mol Neurodegener 6: 23. [PubMed: 21426580]
30. Rajamaki K, Lappalainen J, Oorni K, Valimaki E, Matikainen S, et al. (2010) Cholesterol crystals activate the NLRP3 inflammasome in human macrophages: a novel link between cholesterol metabolism and inflammation. PLoS One 5: e11765. [PubMed: 20668705]
31. Dai WS, LaPorte RE, Hom DL, Kuller LH, D'Antonio JA, et al. (1985) Alcohol consumption and high density lipoprotein cholesterol concentration among alcoholics. Am J Epidemiol 122: 620–627. [PubMed: 2862791]
32. Ruixing Y, Yiyang L, Meng L, Kela L, Xingjiang L, et al. (2010) Interactions of the apolipoprotein C-III 3238C>G polymorphism and alcohol consumption on serum triglyceride levels. Lipids Health Dis 9: 86. [PubMed: 20716347]
33. Rapp JH, Pan XM, Neumann M, Hong M, Hollenbeck K, et al. (2008) Microemboli composed of cholesterol crystals disrupt the blood-brain barrier and reduce cognition. Stroke 39: 2354–2361. [PubMed: 18566307]
34. Steiner TJ, Rail DL, Rose FC (1980) Cholesterol crystal embolization in rat brain: a model for atheroembolic cerebral infarction. Stroke 11: 184–189. [PubMed: 7368248]
35. Abela GS (2010) Cholesterol crystals piercing the arterial plaque and intima trigger local and systemic inflammation. J Clin Lipidol 4: 156–164. [PubMed: 21122648]
36. Myers RD (1981) Alcohol's effect on body temperature: hypothermia, hyperthermia or poikilothermia? Brain Res Bull 7: 209–220. [PubMed: 6974036]
37. Li H, El-Dakdouki MH, Zhu DC, Abela GS, Huang X (2012) Synthesis of betacyclodextrin conjugated superparamagnetic iron oxide nanoparticles for selective binding and detection of cholesterol crystals. Chem Commun (Camb) 48: 3385–3387. [PubMed: 22245910]
38. Galea J, Armstrong J, Gadsdon P, Holden H, Francis SE, et al. (1996) Interleukin-1 beta in coronary arteries of patients with ischemic heart disease. Arterioscler Thromb Vasc Biol 16: 1000–1006. [PubMed: 8696938]
39. Tedgui A, Mallat Z (2006) Cytokines in atherosclerosis: pathogenic and regulatory pathways. Physiol Rev 86: 515–581. [PubMed: 16601268]

- Elevation of plasma cholesterol, formation of cholesterol crystals, and subsequent activation of NLRP3inflammasome in alcohol intake establishes theepidemiological evidence between alcoholism and incidence of stroke.
- Formation of cholesterolcrystalsin blood samples from alcohol users validates the clinical importance of these findings.
- Distinctive neuropathy around the atherosclerotic lesions indicates vascular inflammation as an initial cause of neuronal degeneration.
- Joint therapy of acetyl-L-carnitine/Lipitor® prevented deposition of cholesterol, formation of cholesterolcrystals, activation of NLRP3, thickening of vessel walls, and elevation of intracranial blood pressure,which streamlinesthe prevention step for health benefits.

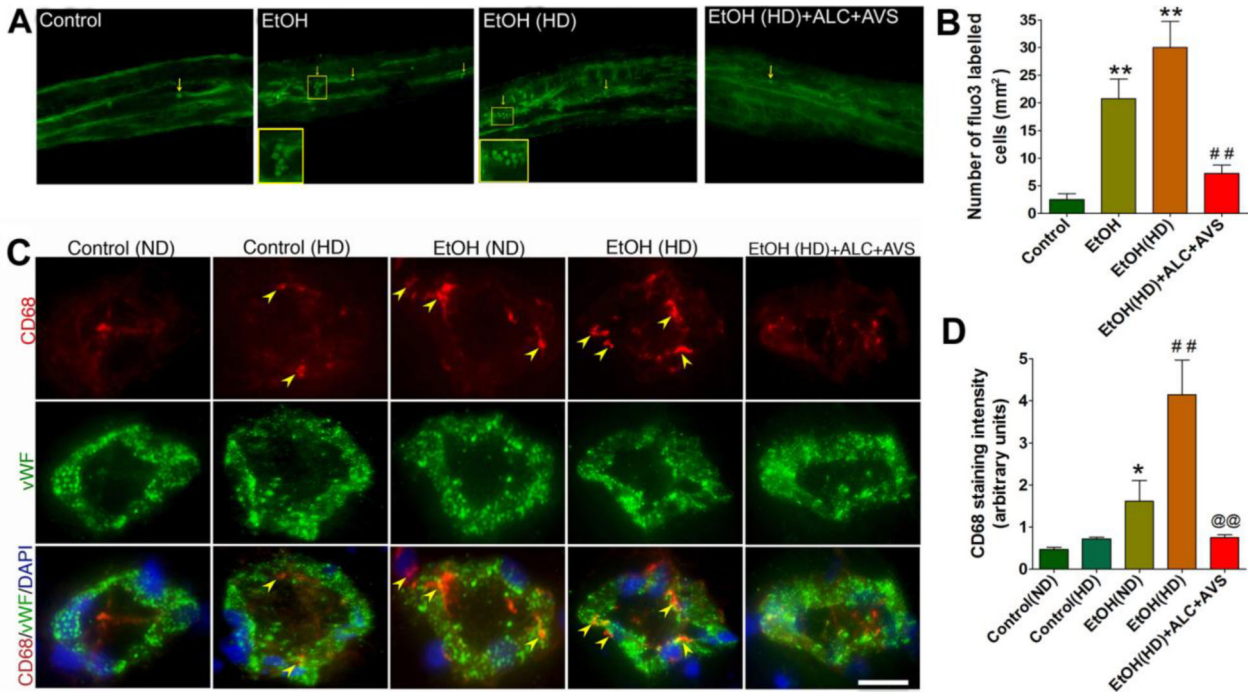

Figure 1: Immune cell adhesion and infiltration in brain arterial vasculature.

(A) Representative images of Fluo-3 labeled macrophages in intact arterioles in control, high-fat diet (HD), ethanol-diet (EtOH), EtOH(HD), EtOH(HD)+ALC+AVS). Cell infiltration on the brain side (basolateral side of arteriole) is highlighted in enlarged images. **(B)** Bar graphs indicate the number of Fluo-3 labeled cells inthe intact microvessels. **(C)** Representative images of CD68 positive cells staining in the capillary endothelium that are co-localized with endothelial marker von Willebrand factor (vWF) and cellular nuclei DAPI in rat brain tissue cross-sections. Arrows indicate infiltrated macrophages and the scale bar is 5 μm. **(D)**Bar graphs indicate CD68 quantification using ImageJ in rat brain microvessels. Data in **(B)**and **(D)** are presented as the mean values (± SEM, N = 5).Statistical significance indicates *p<0.05, **p<0.01 compared with control(ND); ##p<0.01 compared with control(HD), and $^{@@}$p<0.01 compared with EtOH(HD).

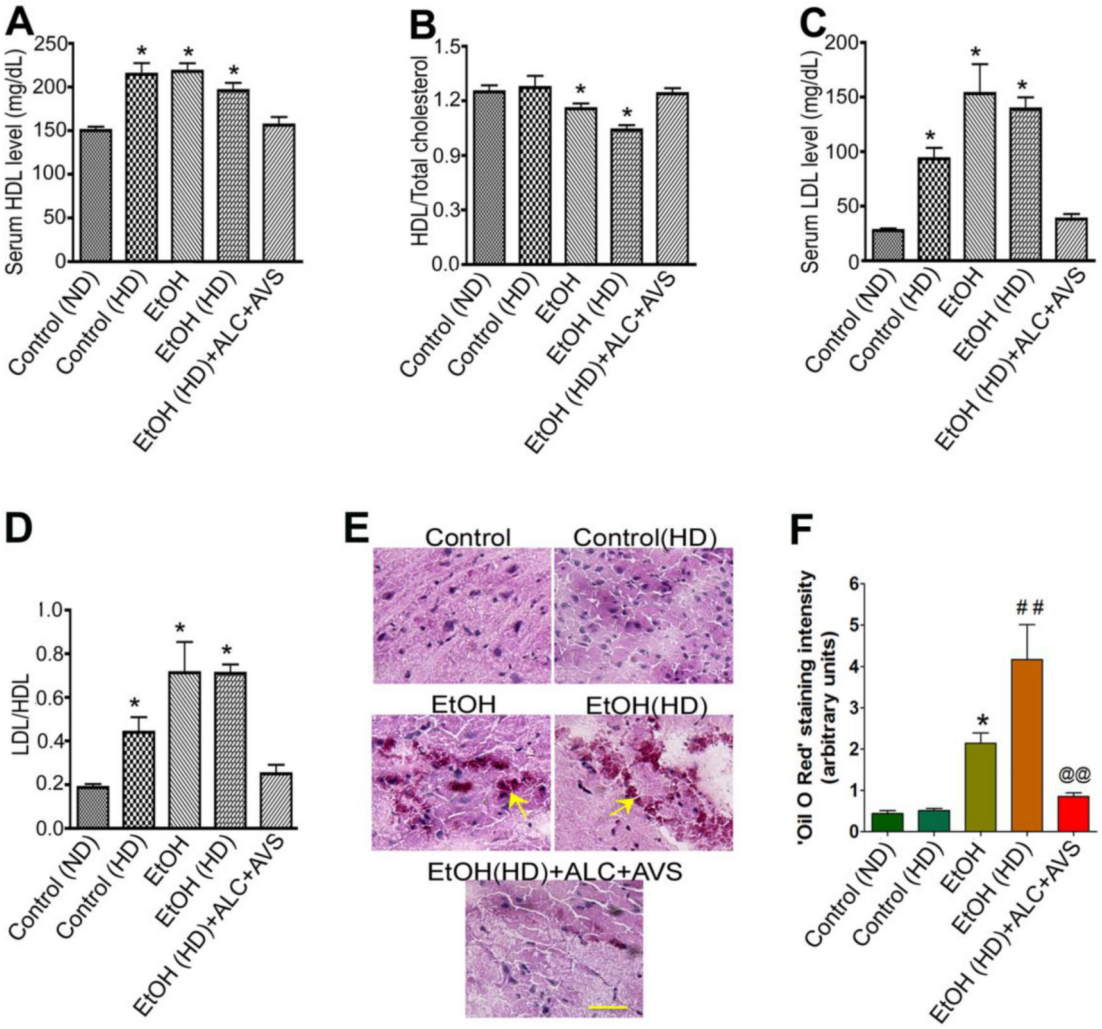

Figure 2: Serum cholesterol levels in chronic alcohol or high-fat diets intake with/without ALC +AVS.

Serum collected from 12–14 weeks pair fed animal were analyzed for total cholesterol and lipoprotein conjugated cholesterol levels. **(A)** HDL levels in serum; **(B)** serum HDL expressed as a ratio of total cholesterol; **(C)** LDL levels in serum, and **(D)** LDL level expressed as a ration of HDL. Statistical significance indicates *p<0.05 compared with control and dataare presented as the mean values (± SEM, N = 5/group). See the composition of normal diet (ND) and high fat diet (HD) in methods section.**(E)**Deposition of cholesterol in brain tissue. The Oil red O staining and microscopy analyses determined the cholesterol deposition in the deep brain frontal corticaltissue sectionsof 8 μm thicknessfrom control, HD, EtOH, EtOH(HD), and EtOH(HD)+ALC+AVS conditions. Scale bar is 5 μm. **(F)**Quantification of 'Oil Red O' staining of cholesterol deposition in the deep brain tissue using ImageJ software in experimental conditions. Data in **(B)**and **(D)** are presented as the mean values (± SEM, N = 5).Statistical significance indicates *p<0.05 compared with control(ND); ##p<0.01 compared with control(HD), and $^{@@}$p<0.01 compared with EtOH(HD).

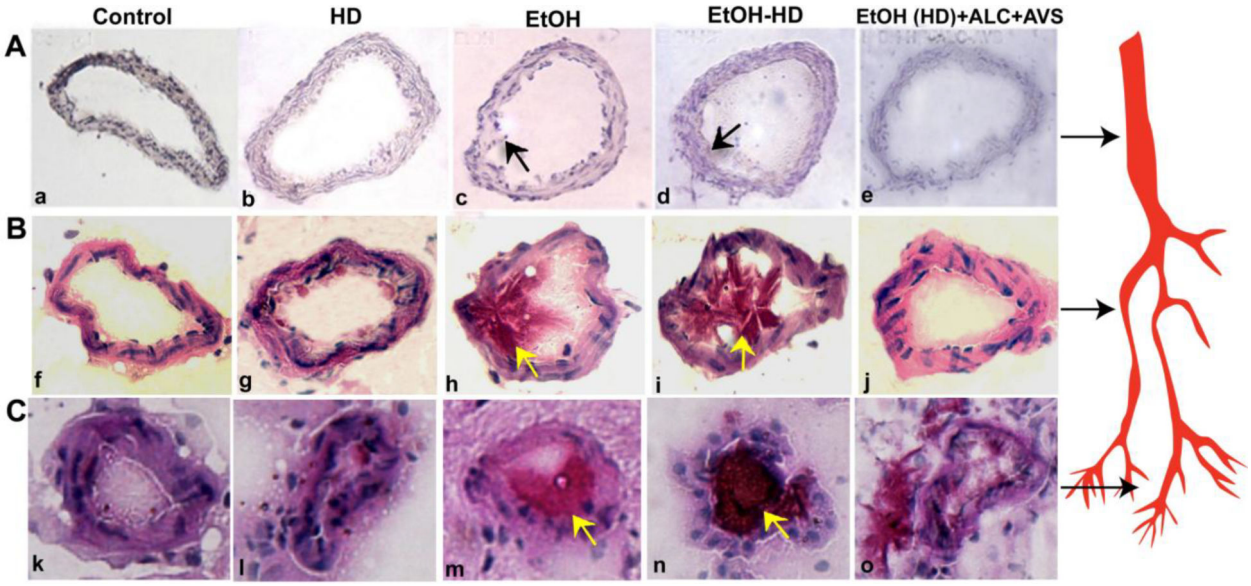

Figure 3: Cholesterol deposition and thickening of the arterial/capillary walls.

Deposition of cholesterol in different segments of the brain vasculature was evaluated by Oil red O staining and microscopy analysesin 8 μm thick brain tissue sections.Representative imaging of cholesterol accumulation and luminal vessel wall thickening in cerebral artery (***A*** *a-e*), arterioles (***B*** *f-j*),and capillary (***C*** *k-o*) from control, high-fat diet (HD), ethanol (EtOH), EtOH(HD), and EtOH(HD)+ALC+AVS. Scale bar is 5 μm, N =5 rats/condition. Arrows indicate the deposition of cholesterol in cerebral artery, arteriole, and capillary. The internal diameters of capillaries in controls or EtOH(HD)+ALC+AVS are 7–10 μm and that of EtOH or EtOH(HD) diets are 5–7 μm. The thickness of the capillary, arteriole or arterial walls in experiment conditions is about 2–3 μm and that of control is about 1–2 μm. The internal diameters of arterioles are about 25 – 40 μm and that of arteries range from 50 – 75 μm. Arrows on the right side of the figure indicate the cerebral artery, arteriole, and capillary segmentation.

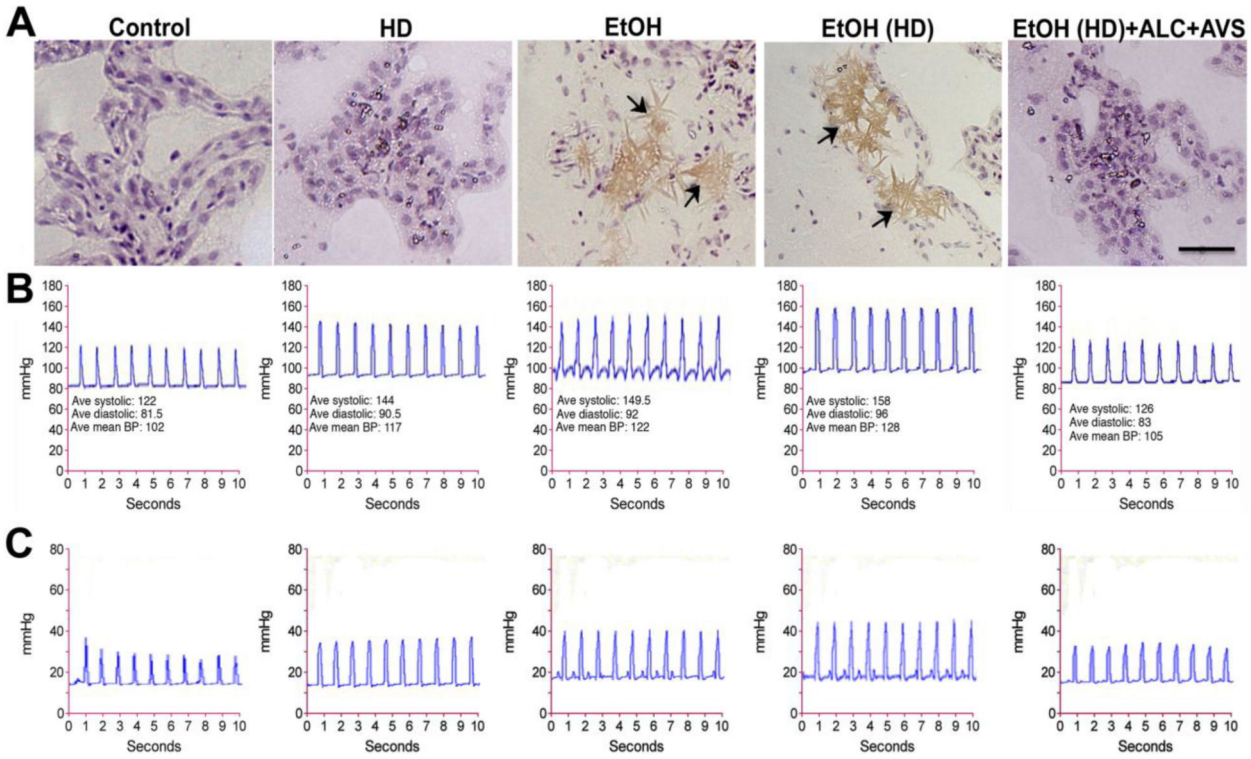

Figure 4: Normalization of plasma cholesterol prevents formation of cholesterol crystals and hypertension.

(A) Hematoxylin and Eosin (H and E) staining of the whole brain tissue sections shows the formation of cholesterol crystals in mid-frontal capillaries of alcohol diet consumed rats only. **(B)** The cardiovascular and **(C)** the intracranial systolic and diastolic blood pressure monitored by 1.2F pressure catheter sensor probe. Note that reduction of arterial/capillary cholesterol levels and CCs formation by ALC+AVS effectively normalized the intracranial blood pressure of alcohol-high fat diet consumed animals to that of control levels. The changes in blood pressure of HD, EtOH, or EtOH(HD) conditions are statistically significant ($p<0.05$) compare to control or EtOH(HD)+ALC+AVS condition.Scale bar is 5 μm, N = 5 animals per condition.

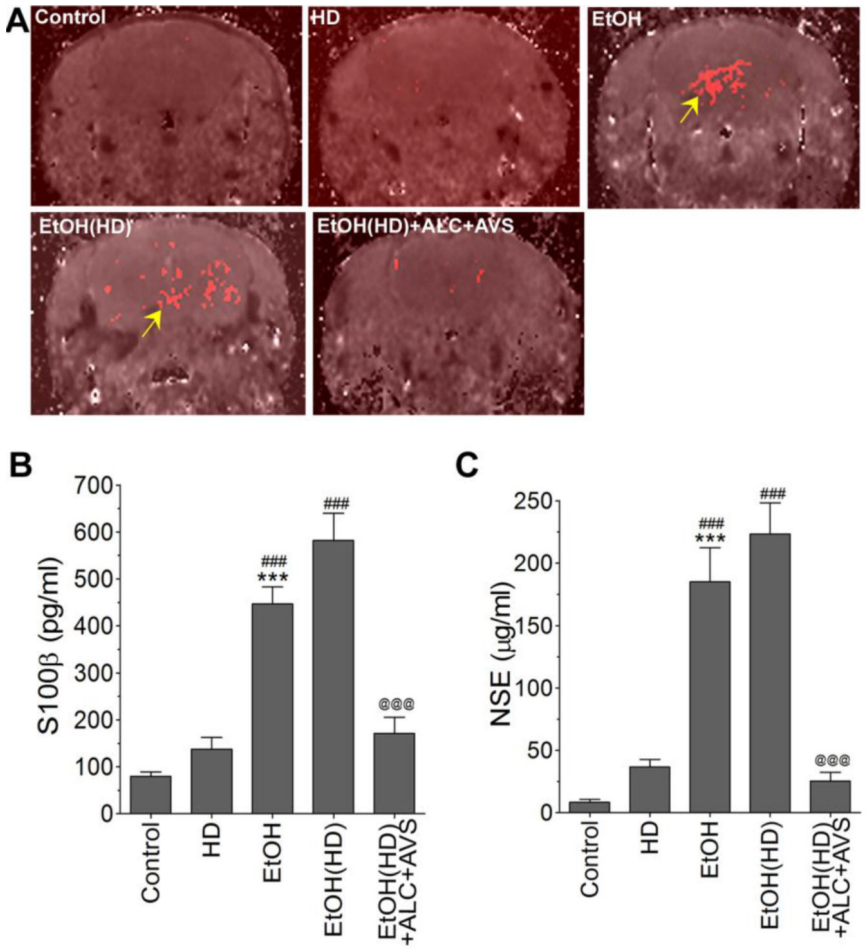

Figure 5: Magnetic resonance brain imaging and BBB permeability assays confirm the leakiness of the BBB due to atherosclerotic lesions in alcohol consumed animals.

(A) Brain infarct volume assessed by MRI gadolinium leakage in control, EtOH, EtOH(HD) and EtOH(HD)+ALC+AVS diets ingested animals. Arrows indicate the atherosclerotic leakage as demonstrated by gadolinium permeability. **(B-C)**Leaking out of brain matters into the circulation as a result of atherosclerotic lesions was assessed by ELISA assay kits. **(B)** Detection of S100β in blood serum suggests the leaking out of astrocytic protein marker into the circulation, and **(C)** detection of NSE in serum suggests the leaking out of brain matter neuronal specific enolase into the circulation. Statistically significant ***p<0.001 compared with control(ND); $^{###}$p<0.001 compared with control(HD); and $^{@@@}$p<0.001 compared with EtOH(HD). Resultsare presented as the mean values (± SEM, N = 5).

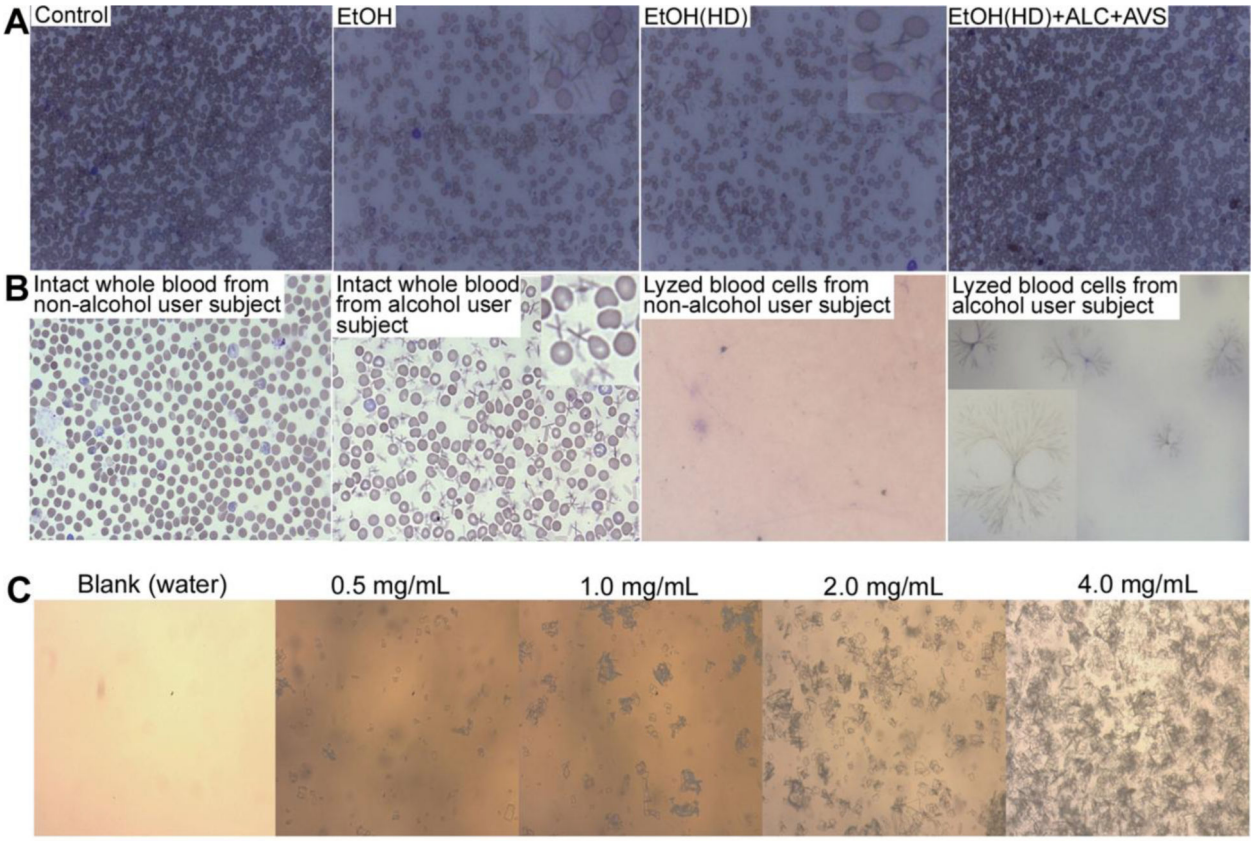

Figure 6: Giemsa staining and microscopy detection of CCs in human whole blood samples and kinetic profile of CC formation.

(A) Detection of CCc in rat whole blood samples from EtOH normal diet (ND) or EtOH high-fat diet (HD) intake compare to control or EtOH(HD)+ALC+AVS diet consumption where CCs were not observed. **(B)***First two left images*: Distinctive presence of CCs in intact whole blood sample from alcohol user human subjects compare to non-alcohol user. *Last two right images*: Clusters of long branching CCs aggregates in lyzed whole blood sample from alcohol user compare to non-alcohol user (magnification 20×). Inserts show the enlarged image of CCs in blood cells (magnification 40×). Data are representative image from N = 6/condition.**(C)** Threshold of CC formation with varying concentrations of cholesterol (0.25 – 4.0 mg/ml) incubated for 2 hours in 1% of ethanol at 37°C. A concentration of 0.25 mg/ml did not yield any traces of CCs.

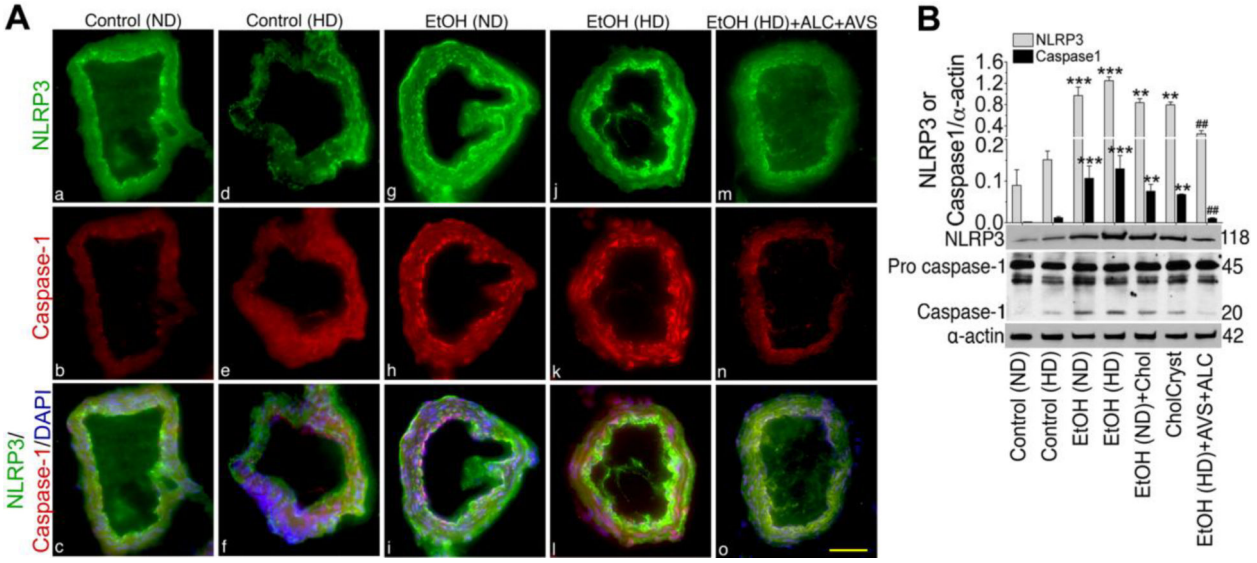

Figure 7: Ethanol induces NLRP3 inflammasomes and activates caspase-1 in rat brain capillaries.

(A). Rat brain capillarystaining of NLRP3 inflammasomes (**green**, A-a,d,g,j,m) and caspase-1 (**red**, A-b,e,h,k,n) merged with DAPI (**blue**, A-c,f,i,l,o) in normal control diet (ND), high-fat diet (HD), EtOH(ND), EtOH(HD), and EtOH(HD)+ALC+AVS conditions. Scale bar indicates 5 μm in all panels. (**B).** Western blot analysis of NLRP3 and caspase-1 (pro- and mature- caspase) in protein extracted from brain microvessels of chronically administered (12–14 weeks)ND, HD, EtOH(ND), EtOH(HD), and EtOH(HD)+ALC+AVS diets consume rats, or infusionof cholesterolin EtOH(ND) consume rat, or infusion of powdered cholesterol crystals(CholCryst) in control rats.Cholesterol or CholCryst was infused through the catheters implanted into the right common carotid artery. Bar graph results are expressed as ratio of NLRP3 or caspase1 to that of α-actin normalization. Data are presented as mean (±SEM; N = 5). *p<0.05, **p<0.01, ***p<0.001 vs control; $^{\#}$p<0.5, $^{\#\#}$p<0.01 vs EtOH (second bar).

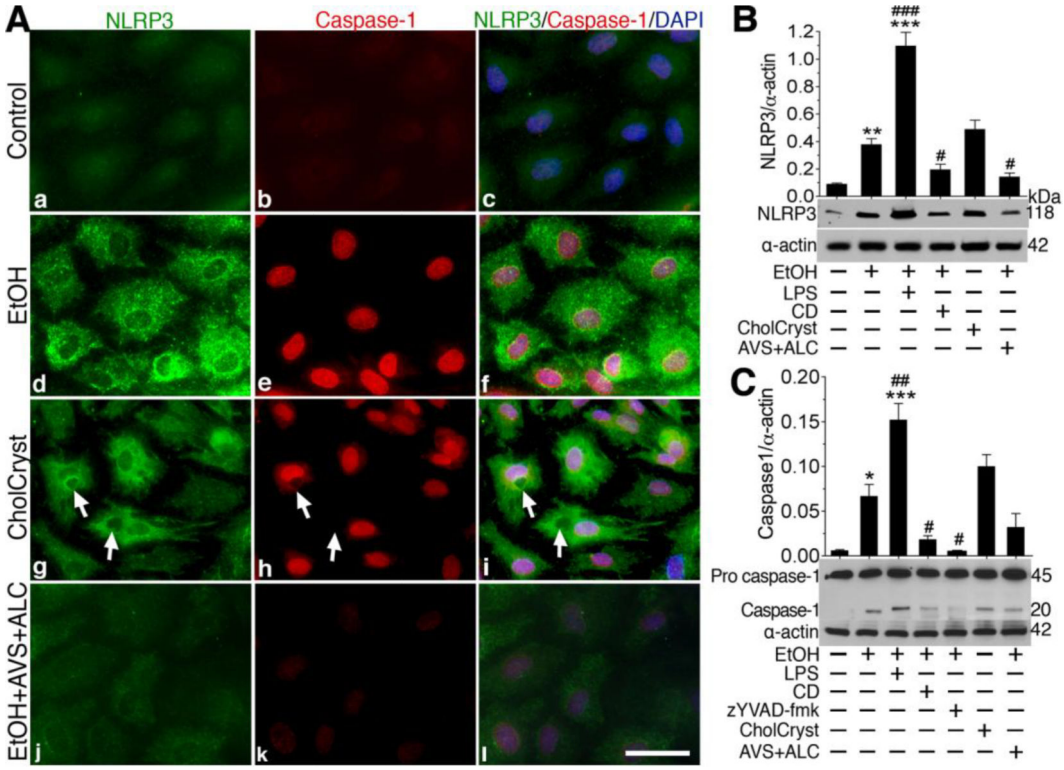

Figure 8: Cholesterol crystals or ethanol activates NLRP3 inflammasomes and caspase-1 in brain endothelial cell culture.

(A) Immunocytochemistry of NLRP3 (green) and caspase-1 (red) merged with DAPI (blue) are shown in untreated, 24 hours 50 mM EtOH, Cholesterol Crystals (CholCryst, 1 mM), and EtOH+ALC (ALC=1 mg/ml) treated hBECs. Scale bar indicates 20 μm in all panels. **B-C)**Western blot analysis of NLRP3 (**B**) and caspase-1 (pro and mature) (**C**) in 24 hours of EtOH (50 mM), EtOH+LPS (LPS=1 g/mL), EtOH+CD (CD=2 M), EtOH+zYVAD-fmk (zYVAD-fmk, caspase-1 inhibitor, 5 g/ml), CholCryst (1 mM) and EtOH+ALC (ALC=100 M) treated hBECs. Bar graphs show the results that are expressed as ratio of NLRP3 in **B** and caspase1 in **C** to that of -actin bands, and values are mean (±SEM; N = 4). *p<0.05, **p<0.01, ***p<0.001 vs control; $^{\#}$p<0.5, $^{\#\#}$p<0.01, $^{\#\#\#}$p<0.001 vs EtOH (second bar).

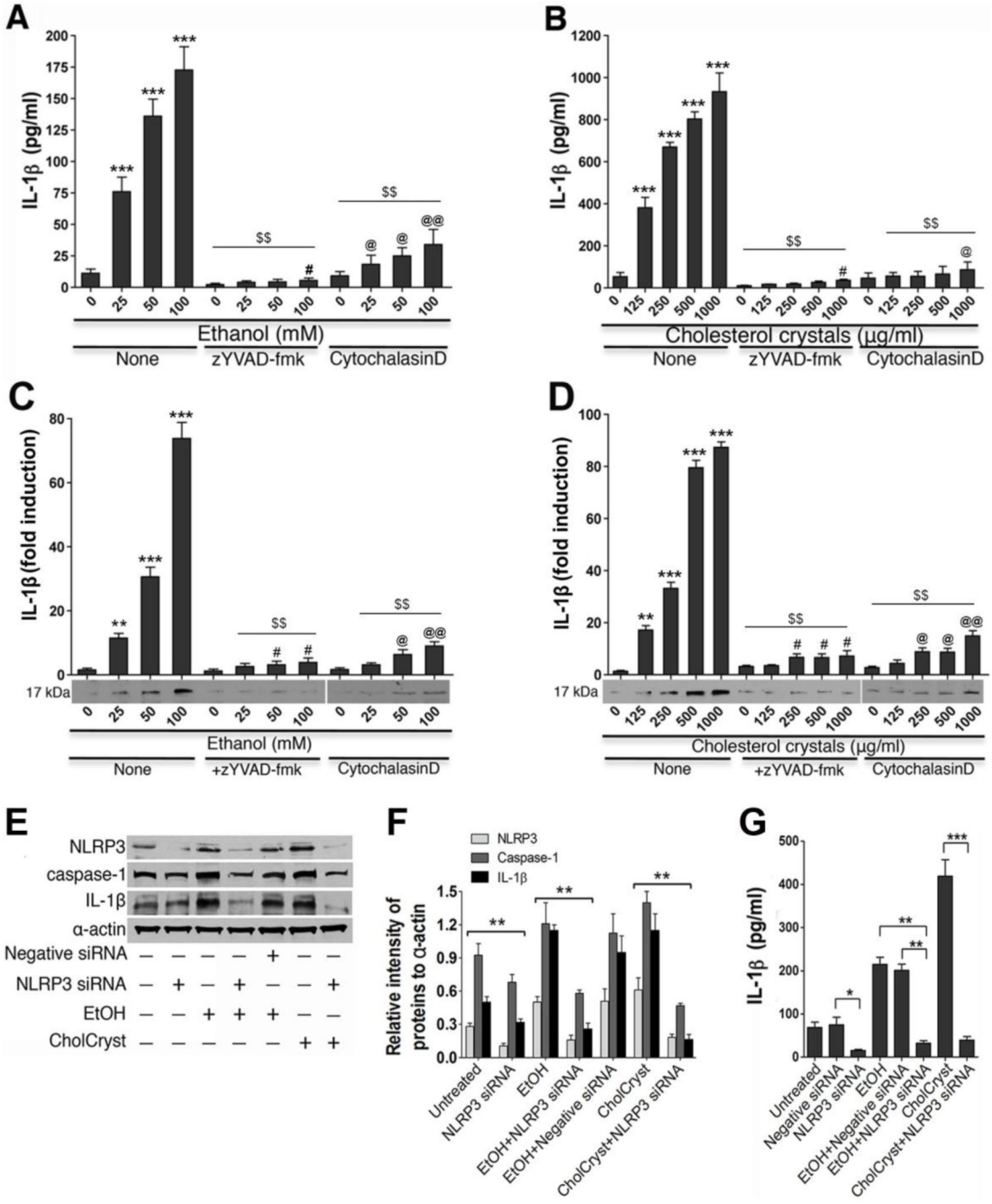

Figure 9 A-D: Dose-dependent effects of ethanol (EtOH) or cholesterol crystals (CCs) on IL-1 secretion due to caspase-1 activation.

The levels of IL-1 secretion in cell culture supernatants and cell lysates were determined by ELISAand Western blot analyses after treating hBECs with various concentrations of EtOH or CCs for 24 hours in the presence or absence of zYVAD-fmk and Cytochalasin D.Dose-dependent effects of EtOH **(A)**and CCs **(B)**onIL-1secretion in hBEC cell culture media determined by ELISA kit. Dose-dependent effects of EtOH **(C)** and CCs**(D)**onIL-1levels in hBEC cell lysates determined by Western blotting. Bar graphs show the relative levels of

IL-1 or immunoreactive band intensity of IL-1 normalized to-actin bandsin respective experiments. Statistical significant **p<0.05,***p<0.001compared with respective controls (O)in EtOH or CCs without zYVAD-fmk or cytochlasinD conditions.#/@p<0.05,@@p<0.01compared with Zero concentration of EtOH or CCs, but in the presence of zYVAD-fmk or cytochlasin D. Results are presented as the mean values (± SEM, N = 6).

Figure 9 E-G: *Silencing the NLRP3 inflammasome gene attenuated the activation of caspase-1 and release of IL-1in hBEC lysates.* Scrambled siRNA hBECs and NLRP3 siRNA hBECs culture were treated with EtOH (50 mM) or CCs (1 mg/ml)for 24 hours for evaluating the changes in NLRP3, Caspase-1 and IL-1 levels. **(E)** Immunoreactive band representative of NLRP3, Caspase-1, IL-1 and -actin in hBEC lysates from various experimental conditions. **(F)** Quantification of NLRP3, Caspase-1, or IL-1immunoreactive bands to that of - actin in hBEC lysates. **(G)** Changes in the levels ofIL-1 in hBEC culture supernatants from respective experimental conditions. Statistical significant *p<0.05 and **p<0.01 compared with corresponding bars. The resultsare presented as the mean values (± SEM, N = 4).

Table 1:

Antibodies source, catalogue numbers, and dilutions factors for immunohistochemical staining and western blotting analyses

Antibody	Marker for	Company	Catalogue #	Dilution for IHC	Dilution for WB
von Willibrand Factor (vWF)	Endothelial cells or microvessels	Abcam	ab11713	1:150	--
NLRP3	NLRP3 inflammasomes	Lifespan Biosciences	LS-C148764	1:250	1:1000
IL-1β	IL-1β	Abcam	ab2105	--	1:1000
α-actin	α-actin	EMD Millipore	ABT1487	--	1:1000
CD68	CD68	EMD Millipore	MABF216	1:250	--
caspase-1	caspase-1	Abcam	ab108362	1:500	1:2000
p-Tau	Phosphorylated Tau	Abcam	ab109390	1:250	--

Table 2.

Demographics of Alcohol Use Disordered Subjects and Controls in whom Blood was Sampled.

In human subjects, control subjects were somewhat younger than the AUD group, but average ages were within 10 years. There were a similar number of men and smokers in both groups. AUDIT scores were by design substantially elevated among the AUD subjects compared to controls. Neither subjects nor controls had evidence of active comorbid conditions by history and physical exam, and routine laboratory values, including a complete blood count and complete metabolic profile were within normal limits as criteria for participation in these investigations.

	Alcohol Use Disordered Subjects, N=10	Control Subjects, N=10	P value
Age in years	47±6	39±11	0.06
Sex, % men	70%	90%	0.96
Current Smokers, %	60%	40%	0.66
AUDIT Score	30±8	2±2	<0.0001